Journal of Physics: Conference Series **741** (2016) 012118 doi:10.1088/1742-6596/741/1/012118

Enhanced photoluminescence efficiency in AlGaN quantum wells with gradient-composition AlGaN barriers

E A Shevchenko, D V Nechaev, V N Jmerik, V Kh Kaibyshev, S V Ivanov and A A Toropov
Ioffe Institute RAS, Saint Petersburg 194021, Russia

Abstract. We present photoluminescence studies of $Al_xGa_{1-x}N/Al_yGa_{1-y}N$ ($y = x+0.3$) quantum well (QW) heterostructures with graded Al content in barrier layers, emitting in the range 285–315 nm. The best-established internal quantum efficiency of the QW emission is as high as 81% at 300 K, owing to enhanced activation energy of charge carriers and exciton binding energy in the QW heterostructure with optimized design.

1. Introduction

AlGaN alloys are widely considered as the most promising materials for design and manufacturing of optoelectronic devices for deep ultraviolet spectral range. The emission efficiency in III-N films grown on commercially available lattice-mismatched sapphire substrates is, however, limited by the emergence of high density of extended and point defects. Under the circumstances, fabrication of the $Al_xGa_{1-x}N$-based heterostructures with high internal quantum efficiency essentially relies on the realization of enhanced fluctuating localization potential, which suppresses charge carriers transport towards non-radiative recombination centers [1]. Provided the activation energy of localized carriers is big enough (e.g. $> 2k_BT$ at 300 K), a relatively high internal quantum efficiency can be achieved even in the structures with the typical defect density exceeding 10^9 cm^{-2}. A convenient measure of the structure internal quantum yield at room temperature is the relative internal quantum efficiency (RIQE) defined as the ratio of photoluminescence (PL) integrated intensities at room and low temperatures I^{RT}/I^{LT}. In particular, Shatalov *et al*. [2] reported the best-known RIQE value of about 70%, evaluated under above-barrier excitation conditions in AlGaN multi-QW structures emitting below 300 nm.

In this paper, we demonstrate an optimized AlGaN single-QW structure grown on *c*-sapphire, emitting near 300 nm with the RIQE of at least 81% under resonant (below-barrier) excitation conditions. Theoretical and technological optimization was performed in order to achieve enhanced electron and hole activation energies both in the vertical direction (along the c-axis) and in the QW plane. Gradient-composition $Al_yGa_{1-y}N$ barriers were introduced in the structures in order to improve collection in the $Al_xGa_{1-x}N$ QW ($x<y$) of the carriers photoexcited within the barriers. Nevertheless, a pronounced difference in the RIQE measured under either above- or below- barrier excitation indicates emergence of noticeable nonradiative losses, which accompany carrier transport within the barrier layers.

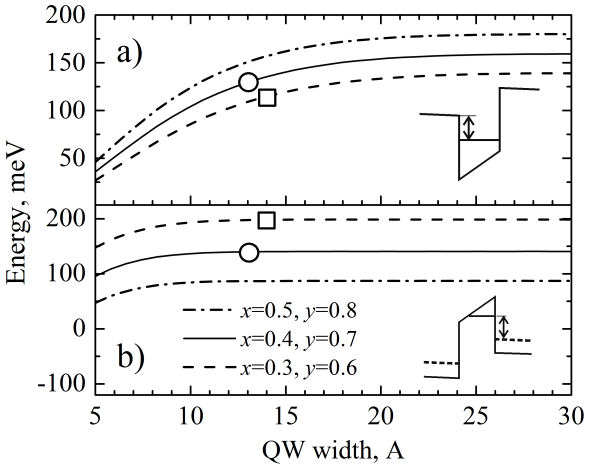

Figure 1. Electron (a) and hole (b) activation energies, calculated as a function of QW width for $Al_xGa_{1-x}N/Al_yGa_{1-y}N$ ($y = x+0.3$) QWs with various combinations of the alloy composition in the QW and barrier layers. Square and circle marks, respectively, indicate parameters of sample A and sample B. The inserts illustrate QW band line-ups.

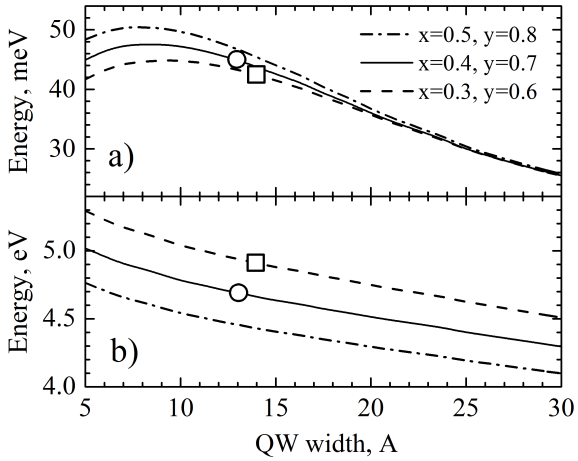

Figure 2. Exciton binding energy (a) and exciton resonance energy (b), calculated as a function of QW width for $Al_xGa_{1-x}N/Al_yGa_{1-y}N$ ($y = x+0.3$) QWs with various combinations of the alloy composition in the QW and barrier layers. Square and circle marks, respectively, indicate parameters of sample A and sample B.

2. Samples design and experiment

2.1. Theoretical simulations

In order to optimize design of the QW structures we estimated the activation energy of carriers as well as parameters of the QW exciton as a function of the QW width. For this aim, band structure and hole effective masses in AlGaN alloys were obtained using a 6-band *kp* model [3], implying pseudomorphic growth with the in-plane lattice constant of an AlN buffer. The QW potential profile was obtained in the approximation of a uniform electric field induced by both spontaneous and piezoelectric polarizations in the pyroelectric compounds with wurtzite crystal structure. We used a transfer matrix method to calculate single-particle energy states and wave functions of electrons and holes, while exciton parameters were evaluated variationally in the approximation of independent excitons by means of a two-parameter trial wave function [4]. All material parameters were taken from [5] besides valence band deformation potentials of AlGaN, which were linearly extrapolated from those of GaN and AlN reported in Refs. [6,7].

Figure 1 shows the activation energies of electrons and heavy holes calculated for three combinations of the alloy composition in the QW and barrier layers in the $Al_xGa_{1-x}N/Al_yGa_{1-y}N$ QW, namely (x=0.3, y=0.6), (x=0.4, y=0.7), and (x=0.5, y=0.8). The difference $y - x = 0.3$ is chosen to achieve reasonably large band offsets at the QW interfaces, while keeping as low Al content in the barrier layers as possible that is a necessary condition of the reliable *p*-doping in respective light emitting diode (LED) structures. The activation energies are obtained as the energy gap between the ground electron (hole) QW energy level and the bottom (top) of the lowest (topmost) band in the barriers (see insertions in Figure 1). For the considered elastic strain conditions, crossing of the heavy-hole and split-off valence bands occurs in $Al_xGa_{1-x}N$ slightly above $x = 0.6$. Therefore, in all three cases, the upper valence band in the QW alloy is the heavy-hole one. The upper valence band in the $Al_yGa_{1-y}N$ barriers is the heavy-hole band for $y = 0.6$, while for two other composition combinations the topmost valence band is the split-off one. The former situation always corresponds to TE polarized emission needed for efficient operation of surface-emitting LEDs [8]. For $y > 0.6$, the TM polarized emission can take place for thin enough QWs when the heavy-hole quantum confined energy level is pushed down be-

low the top of the split-off band in the barriers. This corresponds to type-II band line-ups and negative hole activation energy. For the chosen parameters, however, this situation does not come true even in the thinnest QWs.

The activation energy of electrons increases with the increase of both QW width and Al content. Even in case of (x=0.3, y=0.6) the activation energy is larger than 60 meV at the QW width exceeding 10 Å, which is twice greater than k_BT at room temperature. The activation energy of holes also increases with the increase of the QW width but decreases with the increase of the Al content. For thick enough QWs (thicker than 10 Å), it exceeds 60 meV even for the combination (x=0.5, y=0.8) with the largest chosen Al content. Note that a further increase of the Al content results in a fast reduction of the hole activation energy and for $x > 0.6$ it becomes negative for any QW width. Figure 2 shows the exciton binding energy (Figure 2 (a)) and exciton resonance energy (Figure 2 (b)) calculated versus QW width for the same composition combinations. To evaluate emission energy of the localized QW excitons one should take into account the Stokes shift, which owes to the exciton localization by fluctuations of the QW width and composition. Even for an ideal QW the Stokes shift should be larger than the energy relevant to a single-monolayer (~2.5 Å) thickness fluctuation, which can be estimated from Figure 2 (b) as 100–200 meV depending on the QW width. Then, one can expect the exciton emission wavelength to be below 300 nm (above 4.13 eV) for all considered composition combinations, provided the QW width is below 15–20 Å. Note that the exciton binding energy strongly increases in the thinnest QWs (see Figure 2 (a)) that is also favorable for light emission due to the additional enhancement of the carriers activation energy [2].

To sum up the above analysis, we declare the optimized parameters limits as 10–15 Å for the QW width and x = 0.3–0.4 for the Al content in the QW. Within these limits, both electron and hole activation energies exceed 100 meV, exciton binding energy exceeds 40 meV, the emission wavelength is below 300 nm, and the Al content in the barriers does not exceed y = 0.6–0.7.

2.2. Experimental techniques

Following the performed analysis, we have grown two optimized QW structures by plasma-assisted molecular beam epitaxy on a *c*-sapphire substrate. Intended parameters of these samples (named further as A and B) are Al content of (x=0.3, y=0.6) and (x=0.4, y=0.7) and QW widths of 14 and 13 Å, respectively. Sample A represents the design with the smallest possible Al content in the barrier layers, which nevertheless secures reasonably high band offsets at the QW interfaces and the exciton emission energy below 300 nm (see Figs. 1 and 2). Sample B is designed to provide a shorter emission wavelength at the expense of larger Al content in both QW and barriers. Both samples possess a 2 μm thick AlN buffer containing six 3.5 nm thick GaN layers aimed to reduce threading dislocations density in the active region [9]. The density of threading dislocations was estimated from XRD measurements as 6.9×10^9 cm^{-2} and 4×10^9 cm^{-2} of edge dislocations, and 9×10^8 cm^{-2} and 7×10^8 cm^{-2} of screw dislocations for samples A and B, respectively. The active region itself consists of a 32 nm thick $Al_yGa_{1-y}N$ barrier, $Al_xGa_{1-x}N$ QW, a 65 nm thick $Al_zGa_{1-z}N$ graded barrier layer ($z = y \rightarrow y+0.3$), and a 10 nm thick AlN cap layer. Digital sub-monolayer epitaxy technique was used to form the QW as a superlattice composed of several sub-monolayer thick sheets [10,11]. The rotation period of substrates was set to 3 seconds for the growth of barriers and to 7 seconds during the QW growth. Due to the ununiformed distribution of metal and nitrogen fluxes across the substrate the slower rotation speed leads to additional alloy composition disordering within the QW layer [12].

Time-integrated PL spectra were measured in the grown samples in a wide temperature range between 10 and 300 K, using harmonics of a femtosecond Ti-sapphire laser (Coherent MIRA 900) as excitation and an OceanOptics QE65Pro spectrometer for registration. We used the fourth and the

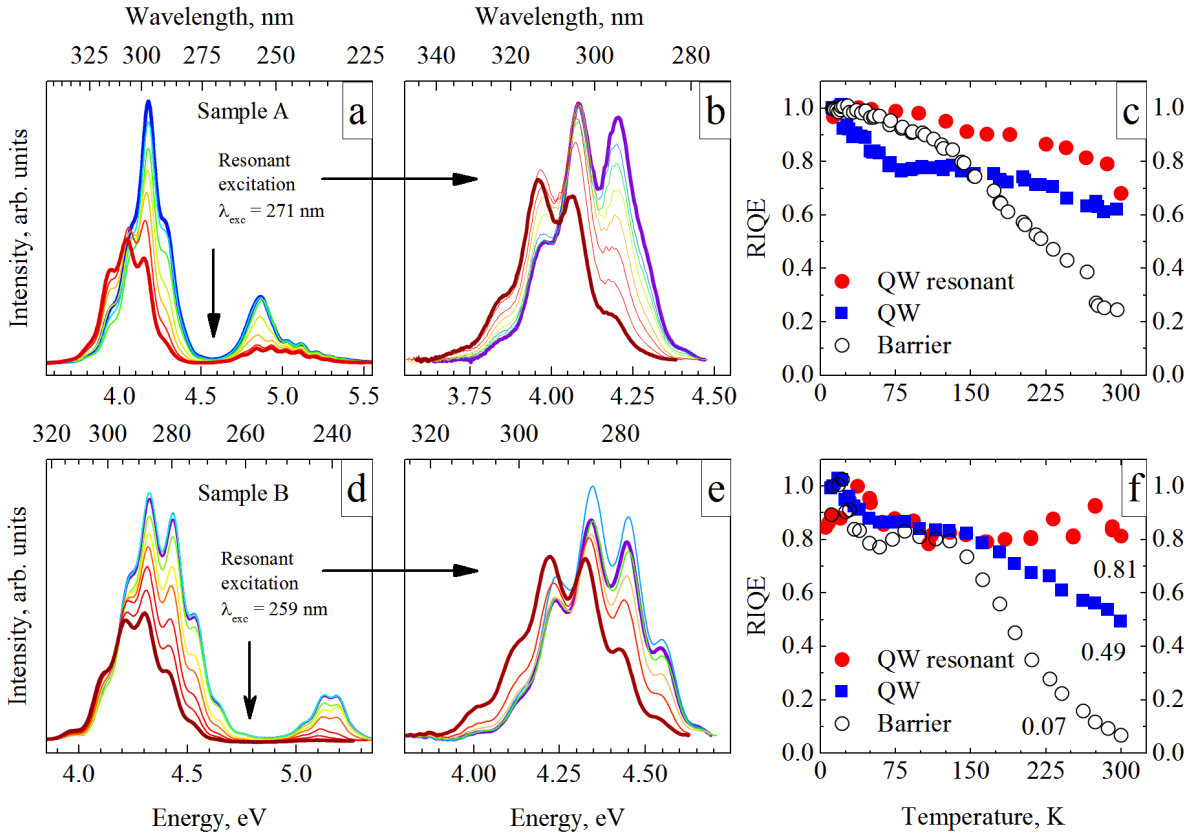

Figure 3. PL spectra of samples A (a, b, c) and B (d, e, f) measured at different temperatures under above-barriers (a, d) and below-barriers (b,e) excitation. RIQE of samples A (c) and B (f) obtained under both excitation modes.

third harmonics of the laser in separate measurement series to excite either barriers or QW, respectively.

3. Results and discussion

The PL spectra measured in both samples are qualitatively similar. Under the excitation by a 210 nm laser line (forth harmonic) the spectra demonstrate two relatively wide separate peaks assigned to the emission of localized excitons in QWs and barriers (Figs. 3 (a) and 3 (d)). In agreement with the intended design, the QW PL peak emerges in Sample A near 300 nm, while in Sample B it shifts toward shorter wavelengths. The whole PL signal is periodically disturbed by light interference defined by reflections from the structure surface and from the interface with the sapphire substrate. Both PL peaks survive up to 300 K, however, the temperature-induced quenching of the QW PL intensity is weaker than that of the barriers. In particular, the ratio of the spectrally-integrated intensities of the QW and barrier peaks (I_{QW}/I_B) decreases with the temperature increase from 28% and 11% to 7% and 1% for samples A and B, respectively (see Figs. 3 (c) and (f)). Since the AlN cap layer and the gradient in the barrier potential profile prevent transport of the photoexcited carriers toward the structure surface and their subsequent surface-induced recombination, we conclude that the drop of the I_{QW}/I_B ratio should be due to the temperature-activated transport of the photoexcited carriers toward QW and, probably, due to their enhanced rate of non-radiative recombination inside barriers as compared with that in QW. In particular, this difference might owe to the enhanced carriers localization within the QW plane, originating from the QW interface roughness and compositional modulations.

Figures 2 (b) and (e) show the series of the PL spectra measured under the resonant (below-barrier) QW excitation by a third laser harmonic. For both samples, the RIQE value of the QW PL for this excitation regime is higher than that under the above-barrier excitation (Figures 2 (c) and (f)). In sample A, the difference between the RIQE curves obtained under different excitation modes first increases with the temperature rise, reaches ~20% at 75 K, and is roughly constant at higher temperatures. Generally, this behavior indicates temperature independence of the additional losses in the barrier layers above 75 K. In Sample B, the behavior is qualitatively different: The difference between the RIQE curves is negligible below ~175 K and drastically increases above this temperature. The distinction between the two samples relies, probably, on varies particular distribution of defects there and is not completely understood at present. Nevertheless, the higher RIQE values observed under the resonant excitation at elevated temperatures clearly indicate emergence of additional non-radiative losses during the carriers transport within the barrier layers.

This observation implies that the true RIQE value of the QW PL is that measured under the resonant excitation. Compare Figs. 3 (c) and (f), one can conclude that the highest RIQE is observed in Sample B. Exact defining of this value is hampered by certain oscillations of the RIQE temperature dependence, originating, most probably, from interplay of the temperature-induced red shift of the whole PL line and the superimposed oscillating interference pattern. Still in case of the worst estimation the RIQE in Sample B is as high as 81%.

4. Conclusions

We have demonstrated the successful design optimization and technological implementation of improved AlGaN based QW structures emitting below 300 nm. The worst-case estimation of RIQE of the QW PL in the best-optimized sample amounts to 81% that is the best-known result to date.

Acknowledgements

This work was supported by Russian Science Foundation (Project #14-22-00107).

References

[1] Chichibu S F *et al*. 2006 *Nat. Mater*. **5**, 810–816
[2] Shatalov M, Yang J, Sun W, Kennedy R, Gaska R, Liu K, Shur M and Tamulaitis G 2009 *J. Appl. Phys*. **105** 073103
[3] Bir G I and Pikus G E 1974 *Symmetry and Strain-induced Effects in Semiconductors* (New York: Wiley)
[4] Toropov A A, Shevchenko E A, Shubina T V, Jmerik V N, Nechaev D V, Yagovkina M A, Sitnikova A A, Ivanov S V, Pozina G, Bergman J P and Monemar B 2013 *J. Appl. Phys*. **114** 124306
[5] Vurgaftman I and Meyer J R 2003 *J. Appl. Phys*. **94** 3675
[6] Ishii R, Kaneta A, Funato M, Kawakami Y and Yamaguchi A A 2010 *Phys. Rev. B* **81** 155202
[7] Ishii R, Kaneta A, Funato M and Kawakami Y 2013 *Phys. Rev. B* **87** 235201
[8] Northrup J E, Chua C L, Yang Z, Wunderer T, Kneissl M, Johnson N M and Kolbe T 2012 *Appl. Phys. Lett*. **100** 021101
[9] Jmerik V N, Lutsenko E V and Ivanov S V 2013 *Phys. Status Solidi* A **210** 439–50
[10] Zhmerik V N, Mizerov A M, Shubina T V, Sakharov A V, Sitnikova A A, Kop'ev P S, Ivanov S V, Lutsenko E V, Danil'chik A V, Rzheutskii N V and Yablonskii G P 2008 *Semiconductors* **42** 1420
[11] Ivanov S V, Nechaev D V, Sitnikova A A, Ratnikov V V, Yagovkina M A, Rzheutskii N V, Lutsenko E V and Jmerik V N 2014 *Semicond. Sci. Technol*. **29** 084008
[12] Toropov A A, Shevchenko E A, Shubina T V, Jmerik V N, Nechaev D V, Pozina G, Bergman J P, Monemar B, Rouvimov S and Ivanov S V 2016 *Physica Status Solidi* C accepted for publication